Quaternary International 664 (2023) 20–32

Contents lists available at ScienceDirect

Quaternary International

journal homepage: www.elsevier.com/locate/quaint

# Variations of heat availability in the Western Caucasus in the past 1500 years inferred from a high-resolution record of bromine in the sediment of Lake Karakel

Mikhail Y. Alexandrin [a,*], Olga N. Solomina [a], Andrei V. Darin [b]

[a] Institute of Geography, Russian Academy of Sciences, Russia
[b] V.S. Sobolev Institute of Geology and Mineralogy SB RAS, Russia

ARTICLE INFO

*Keywords:*
Climate reconstructions
SR XRF analysis
Lake sediments
Bromine
Heat availability
Western caucasus

ABSTRACT

The Caucasus region lacks climate-sensitive chronologies that are continuous, high-resolution and covering more than several centuries at the same time. This paper presents the first high-resolution curve reflecting the variations of heat availability in the Western Caucasus over the past 1500 years. The chronology of bottom sediment of Lake Karakel is based on the two precisely overlapped sediment cores, constrained by ten $^{14}C$ dates with a temporal resolution of around 3 years. Bromine content in the sediment is interpreted as a proxy for variations of heat availability based on its coherence with the broadleaved tree pollen content in the same deposits. Lake Karakel Br curve showed distinct agreement with hemispheric and regional temperature reconstructions starting from 500 CE, as well as with the tree-ring temperature reconstructions available for the Caucasus. It allowed a constraint of the time frames for the main climatic events in the Western Caucasus during the past 1500 years: Medieval Climate Anomaly (ca. 960–1270 CE) and Little Ice Age with its three separate stages (LIA 1 ca. 1270–1310 and 1370–1410; LIA 2 ca. 1500–1630; LIA 3 ca. 1750–1840). Br-derived variations of heat availability are also supported by the recent cosmogenic glacier moraine dates in the Caucasus.

## 1. Introduction

The history of climate change of the Western Caucasus – the westernmost and most humid part of the Caucasus Mountain system – is still lacking necessary details. Hence the climatic variability of the region lying beyond the scope of instrumental records and historical sources of the last one and a half centuries is obscure. Generally, even the time frames and the magnitude of the major climatic events of the past two millennia, such as Roman Warm Period, Medieval Climate Anomaly and Little Ice Age are far from being robust (Solomina et al., 2016a). Climate conditions during the early and mid-Holocene, including the timing of Neoglacial glacier advances, are currently even more uncertain (Solomina et al., 2015).

Previous studies of bottom sediments of the lakes of the Western Caucasus by Serebryanny et al., (1984), Kvavadze and Efremov (1996) and others are based predominantly on palynological studies of sediment cores. The longest available high-resolution temperature reconstruction for the North Caucasus region based on dendrochronology covers the period 1596–2011 (Dolgova, 2016). The chronology based on the recent Mt. Elbrus ice core covers only 240 years (Kutuzov et al., 2019). For the Western Caucasus, a region abundant in high-elevation lakes, bottom sediments are a vital source of data regarding past variations of climate and environment, since this archive is capable of providing millennia-long chronologies with high temporal resolution.

Recent advances in lake sediment studies of the Caucasus region include the modern varved sediment of Lake Donguz-Orun (Central Caucasus), where the correlations between the sedimentary geochemical data and instrumental parameters were established (Alexandrin et al., 2018), and the sedimentary record of Lake Khuko (Western Caucasus) that covers almost the whole Holocene, yet it is based on low-resolution spore-pollen analysis (Grachev et al., 2020). The present research offers the first known continuous high-resolution sedimentary record in the region.

Technological advance of recent decades enabled sedimentary analyses that are both non-destructive and high-resolution. High-resolution data along with robust chronological control allow for reconstructions of high-frequency climate fluctuations and abrupt events – things becoming increasingly important in context of modern warming and

* Corresponding author. .
*E-mail address:* alexandrin@igras.ru (M.Y. Alexandrin).

https://doi.org/10.1016/j.quaint.2023.05.020
Received 11 January 2023; Received in revised form 23 May 2023; Accepted 27 May 2023
Available online 11 June 2023

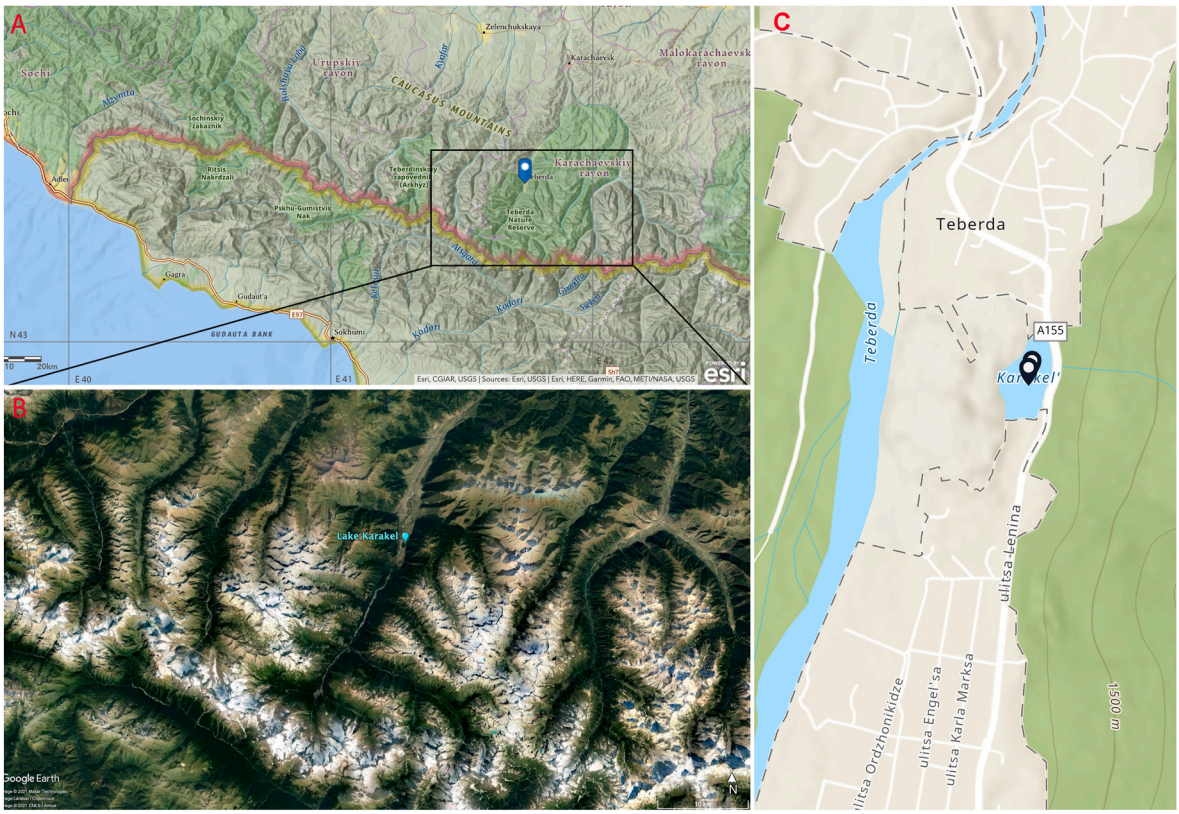


**Fig. 1.** A: Location of Lake Karakel. Image courtesy: ESRI. B: Aerial image of the lake's catchment area. Image courtesy: Google. C: Map of lake's vicinity and the coring locations of the studied cores. Image courtesy: ESRI.

forecasting. Developing and ensuring the efficiency of high-resolution biogenic markers of lake sediments can be crucial for some environments. This work is based on one of the novel biogenic markers – a content of bromine in the lake sediments. We argue that content of bromine in the sediment of Lake Karakel obtained with the use of high-resolution synchrotron radiation x-ray fluorescence analysis can be interpreted as a proxy for variations of heat availability in the region. This assumption is constrained by pollen analysis and supported by the previously established correlations between the content of bromine and instrumental temperature in the Caucasus and in Siberia. In this paper, we aim at creating a one-and-half millennia-long reconstruction of heat availability in the Western Caucasus with a resolution of around 3 years. Inability to calibrate the modern sedimentary data against instrumental meteorological data restricts the creation of a quantitative temperature reconstruction. Yet, the reconstruction of heat availability in the region also yields important knowledge: it helps to constrain the time frames of the main climatic events in the Western Caucasus over the last 1500 years and assess their magnitude – something that was previously not possible.

## 2. Study area

The study area lies in the westernmost part of the Greater Caucasus – is the most elevated and the most humid part of the Caucasus Mountain system. The climate of the Western Caucasus is defined by the region being a barrier between temperate air masses moving southward from the Russian Plain and humid air masses of the Black Sea moving eastward, along with complex mountain orography (Fig. 1A).

Lake Karakel (43°26′12.44″N; 41°44′36.18″E) is situated in the Teberda River valley sourced from the Main Caucasus Range (Fig. 1B). The valley stretches in the SW-NE direction and is around 1200-m wide in the lake's vicinity. The lake lies at the altitude of 1335 m a.s.l., it is elongated along the valley axis with dimensions around 140 x 280 m. Bathymetric surveys demonstrate that the central part of lake's bottom is nearly flat with a mean water depth of 9 m. The slopes of the Teberda Valley surrounding the lake are built up with plagiogranites and granitoids of the Main Caucasus Ridge, the left side of the valley also reveals metamorphic outcrops (State geologic map, 2011).

The lake was most likely formed by damming of glacial runoff by a moraine ridge which can still be traced to the south-west, west and north-west of the lake (Serebryanny et al., 1984). Currently the Lake is closed with a portion of the outflow presumably filtering through the subjacent moraine. The lake is fed by atmospheric precipitation and snowmelt. The surrounding slopes are mainly covered with pine forests with addition of birch, oak, beech, elm and hornbeam. The tree limit reaches 2300 m a.s.l. at the northern slopes and 2600 m a.s.l. at the southern slopes.

Instrumental meteorological records of Teberda started in 1926. The mean annual temperature is 6.9 °C, the winter is mild with mean temperature in January of 3.2 °C, the summer is moderately warm with mean temperature in July of 16.4 °C. Annual precipitation is around 700 mm with maximum precipitation during the summer season. The mean wind velocity is 1.8 m/s. The lake is currently situated within the residential area of the Teberda settlement being subject to recreational use during the last century.

## 3. Methods

### 3.1. Sediment coring

The first sediment cores of Lake Karakel were retrieved in 2010 (cores Kar-10-1 and Kar-10-2) and 2014 (core Kar-14-1) by fellows of Institute of Geography RAS using a modified piston corer (Nesje, 1992). The corer was mounted on an inflatable catamaran based platform. Coring was performed in the central part of the lake at a water depth of 9 m. Standard non-transparent PVC tubes of the 110-mm diameter were

**Table 1**
Radiocarbon ages for Lake Karakel sedimentary sequence. Calibrated with OxCal 4.4 (Ramsey, 2009)/IntCal20 calibration curve (Reimer et al., 2020).

| Sample lab# | Core | Depth per core, cm | Depth combined, cm | Age $^{14}$C, yr BP (1σ)/ pmc, % | Calibrated 2σ age range (cal. yr BCE/CE) | Calibrated median age (cal. Yr BCE/CE) | Material |
|---|---|---|---|---|---|---|---|
| IGAN-5497 | Kar-14-1 | 7–8 | 7–8 | 100.740 ± 0.292 | 1697-1724; 1812–1836; 1881–1911 | 1825 | bulk TOC |
| IGAN-5496 | Kar-14-1 | 13.5–14.5 | 13.5–14.5 | 340 ± 30 | 1474–1638 | 1561 | bulk TOC |
| IGAN-5493 | Kar-14-1 | 13.5–14.5 | 13.5–14.5 | 725 ± 20 | 1266–1298 | 1280 | terrestrial macrofossil |
| IGAN-5495 | Kar-14-1 | 18–19 | 18–19 | 640 ± 20 | 1290-1326; 1351-1395 | 1360 | bulk TOC |
| IGAN-5494 | Kar-14-1 | 21–22 | 21–22 | 640 ± 20 | 1290-1326; 1351-1395 | 1360 | bulk TOC |
| IGAN-5333 | Kar-10-2 | 6–6.5 | 28.5–29 | 880 ± 20 | 1053-1076; 1156-1120 | 1185 | bulk TOC |
| IGAN-5332 | Kar-10-2 | 12–12.5 | 34.5–35 | 1030 ± 20 | 991–1030 | 1010 | bulk TOC |
| IGAN-5331 | Kar-10-2 | 20–20.5 | 42.5–43 | 1235 ± 20 | 668-742; 772–779; 785-878 | 798 | bulk TOC |
| Poz-42587 | Kar-10-2 | 30–31 | 52.5–53.5 | 1550 ± 30 | 431–587 | 513 | bulk TOC |
| Poz-42588 | Kar-10-2 | 52 | 74–75 | 2235 ± 35 | 391-338 BCE; 326-198 BCE | 278 BCE | bulk TOC |

used to collect the sediment. Three overlapping cores were obtained with the total length of 203 cm. Current paper focuses solely on the upper section (0–80 cm) of the sediment comprised of the cores Kar-10-2 and Kar-14-1.

### 3.2. Laboratory analyses

The cores were subsequently cut in half along the main axis under laboratory conditions. Conventional sedimentary analyses were implemented on one half-core. For both cores Kar-10-2 and Kar-14-1 we measured weight loss-on-ignition (LOI) at 550 °C every 1 cm (Dean, 1974; Heiri et al., 2001) (Fig. 6).

X-ray fluorescence analysis using synchrotron radiation (SR XRF) was performed at the Local and Scanning X-Ray Fluorescence Element Analysis Station of the Siberian Synchrotron and Terahertz Radiation Center with VEPP-3 storage ring as the synchrotron radiation source following the procedures described in (Darin et al., 2013). A monochromatic beam of synchrotron radiation with energy of 21 keV was used. The contiguous blocks 160 mm × 20 mm × 5 mm of samples impregnated with epoxy resin were prepared for the scanning analysis. The concentrations of 25 elements were determined at a resolution of 1 mm: K, Ca, Ti, V, Cr, Mn, Fe, Ni, Zn, Ga, As, Br, Rb, Sr, Y, Zr, Nb, U. The peak areas were recalculated into concentrations using the external standard procedure (Darin and Rakshun, 2013). State Standard Sample of BIL-1 composition (Baikal silt, GSO 7126-94) was used as an external standard (www.igc.irk.ru). The resultant elemental values are expressed in ppm and fully presented in Supplementary material.

### 3.3. Dating and age-depth modelling

The chronology of the Lake Karakel sediment sequence is based on ten $^{14}$C dates (5 per each sediment core Kar-10-2 and Kar-14-1). $^{14}$C measurements were performed by accelerator mass spectrometer (AMS) at the Poznan Radiocarbon Laboratory (Poland) and The Center for Applied Isotope Studies at the University of Georgia (USA) (Table 1). For the samples measured after 2016 the sample graphitization was carried out in the Laboratory of Radiocarbon Dating and Electronic Microscopy of the Institute of Geography RAS (Moscow).

The age–depth model (Fig. 5) was created using R software and the R-code package 'rBacon' using Bayesian statistical framework (Blaauw and Christen, 2011) with the IntCal20 radiocarbon calibration curve of Reimer et al. (2020).

## 4. Results

### 4.1. Core stratigraphy

The composite sedimentary sequence of Lake Karakel is comprised of the three sediment cores and is 203 cm long. Stratigraphic analysis of the cores revealed that the lake's bottom sediment consists of two fundamentally different strata. The sediment depth from 0 to 70–80 cm is represented by dark brown gyttja with mean values of weight loss-on-ignition around 30–50%, while from 80 cm the sediment is comprised of finely laminated beige silty clay reminiscent of proglacial lake sediments with mean values of weight loss-on-ignition around 4–5%. The current paper focuses solely on the upper part the sediment record corresponding to the last 2000 years for which the SR XRF analysis was performed (Fig. 2).

The master-core used for further paleoclimatic implications was created by means of precise correlation of the sediment cores Kar-10-2 and Kar-14-1 (the correlation technique is described in the section 4.3).

### 4.2. X-ray fluorescence element analysis

The results of the SR XRF analysis of the two cores were combined into one following the procedure described in the following section. Namely, most of the resultant chronology is based on the core Kar-14-1 (Fig. 3) with the bottom part added from the core Kar-10-2. The results show a major agreement between the curves of the terrigenous elements (K, Ti, Rb, Zn and others) and the inverse behavior of the elements of non-detrital origin (Br, U).

The two visible interlayers at the depths 20–30 mm (Kar-10-2) and 200–220 mm (Kar-14-1) and the one around the depth 550 mm (Kar-14-1) are marked with distinctive spikes in the concentrations of terrigenous elements (K, Ti, Rb, Y, Zr, Nb). This could imply turbidite layers with instantaneous accumulation due to an undefined slope process, although the exact nature of these processes is yet to be determined.

### 4.3. Creating a master chronology

The cores Kar-10-2 and Kar-14-1 were first visually combined basing on the distinctive whitish interlayers at the depths 20–30 mm (Kar-10-2) and 200–220 mm (Kar-14-1) (Fig. 2). Along with the $^{14}$C age of the uppermost date of the core Kar-10-2 (880 ± 20 $^{14}$C years at 6 cm depth) that implied that a longer core Kar-10-2 lacked the upper portion of the sediment.

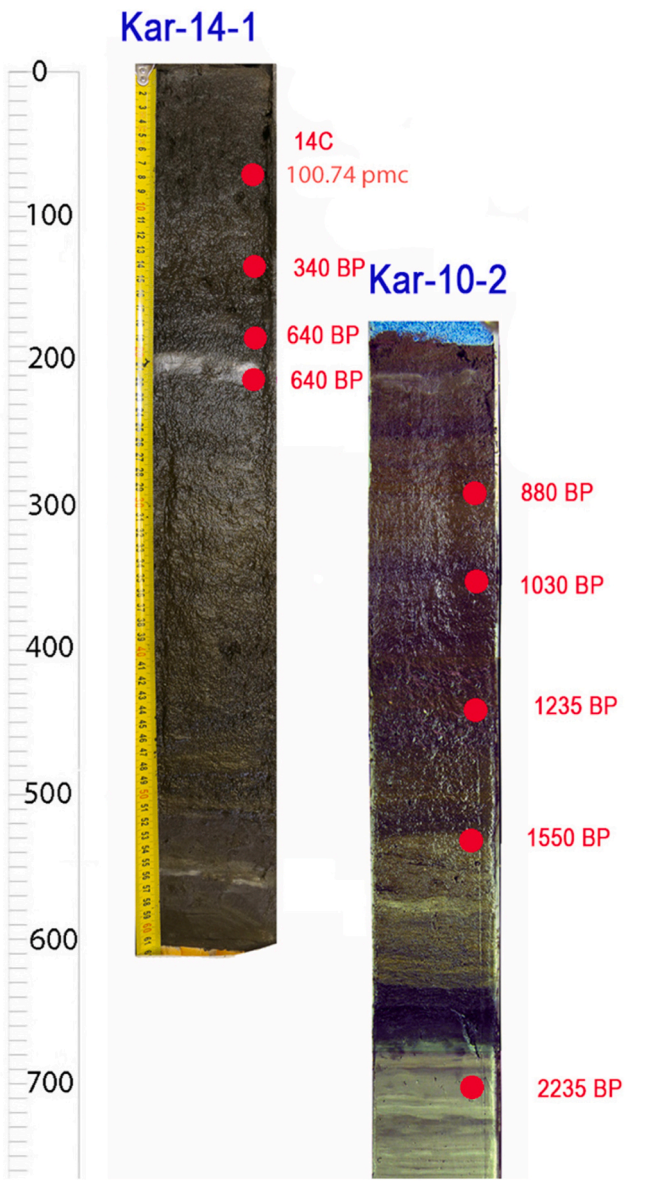


**Fig. 2.** Combined sediment cores of Lake Karakel along with sampling spots for dating and corresponding $^{14}C$ ages. pMC stands for percent modern carbon.

High-precision correlation of the two cores was made possible with the use of the SR XRF scanning results. The aforementioned whitish interlayers in both cores were marked with significant spikes in the concentrations of chemical elements characteristic of terrigenous origin (K, Ti, Rb, Y, Zr, Nb). Fig. 4 shows the profiles for Ti (A) and Rb (B). The best match was achieved with the elongation of the upper core by 1.17 times and offset by 225 mm. The elongation of the upper core is most likely explained by slightly offset coring locations during the field expeditions of 2010 and 2014 with slightly different linear accumulation rates. The two cores were combined in a composite sediment core master chronology with an accumulation rate close to linear throughout the period starting 400 BCE (Fig. 5).

### 4.4. Chronology

The age-depth model (Fig. 5) is based on nine $^{14}C$ dates (sample IGAN-5493 (terrestrial macrofossil) was excluded from the model due to translocation downcore during coring) allows for robust chronological control of the sedimentary analytical data. The model shows a near-linear relation throughout the study period that with a mean sedimentation rate of 2.9 yr/mm or 0.34 mm/yr. Transferring the XRF results from the depth scale into the temporal scale yields the temporal resolution of our chronology of around 3 years (as calculated with the use of rBacon for each of the SR XRF measurements made with 1-mm resolution).

The last part of the chronology is less well constrained: 20 cm of the sediment account for around 750 years (278 BCE-523 CE median age). The bottom $^{14}C$ age is retrieved in the upper part of the minerogenic stratum of the sediment, which might imply a possible hiatus between the two strata. While the bottom part of Lake Karakel sedimentary sequence requires additional dating, the last 1500 years that are the focus of current paper are sufficiently chronologically constrained for the purposes of this study.

## 5. Discussion

### 5.1. Br content as a temperature-sensitive proxy

Bromine exists naturally in several oxidation states, it is also known to form strong covalent bonds with carbon (Gilfedder et al., 2011). Most of the known Br compounds are of marine origin (Croudace and Rothwell, 2015) and Br was widely used to quantify marine organic matter and productivity (e.g., Mayer et al., 1981; Ziegler et al., 2008; Addison et al., 2013) or to determine marine vs freshwater deposition conditions (Mayer et al., 2007; Kalugin et al., 2015; Kandasamy et al., 2018). Bromine was historically perceived to have conservative cycling between the oceans and the continents. Recent studies, though, show that bromine is involved in dynamic geochemical cycle involving bedrock, soils, vegetation and freshwaters (Gilfedder et al., 2011).

Leri et al. (2010) performed a detailed study of the Br cycle in marine sediments. They showed that Br undergoes biogeochemical cycling with natural formation and degradation of organobromine compounds in marine systems. Organobromine compounds represent the dominant form of Br in different sedimentary environments. The connection between bromine and organic carbon in marine sediments is attributable to covalent C–Br bonds (Leri et al., 2010). Leri and Myneni (2012) subsequently studied biogeochemical cycle of Br in terrestrial environments. Br content in terrestrial environments is an order of magnitude less as compared to that of marine environments, yet is traceable with modern analytical techniques, such as XANES spectroscopy (Leri and Myneni, 2012). This research showed the conversion of inorganic bromide to organobromine through natural mechanisms. All Br in isolated humic substances, decaying plant material, and the organic fraction of soils is covalently bonded to carbon, making Br a reliable tracer of organic matter.

A possible connection between the accumulation of Br in freshwater bottom sediments and temperature is far from being completely understood, as is the terrestrial Br cycle itself. Wishkerman et al. (2008) showed a strong dependance of emission of methyl bromide ($CH_3Br$, the most abundant brominated organic compound in the atmosphere) from dried plant matter on bromide content of terrestrial plants and air temperature (emissions were observed to approximately double with every 5 °C rise in temperature). A number of studies provides evidence of Br being a temperature-sensitive paleoclimate proxy, though often indirectly. Phedorin et al. (2000) studied Br in the sediments of Lake Baikal. They applied a spectral analysis to the Br concentration over the last 480 kyr and found that the spectra are similar to those obtained with the oceanic profile of $\delta^{18}O$ (105:41:23:19 kyr). Br is therefore proposed as a "warm" proxy with its concentrations increasing in those layers of the sediment that belong to warmer climates (Phedorin et al., 2000). Bahr et al. (2014) used Br for stratigraphic purposes in their 140 kyr-long chronology, since it was shown that variations of Br closely resemble that of mid and high latitude North Atlantic climate change preserved in stable isotope records.

Br content can be used to trace the provenance of the sediment in the

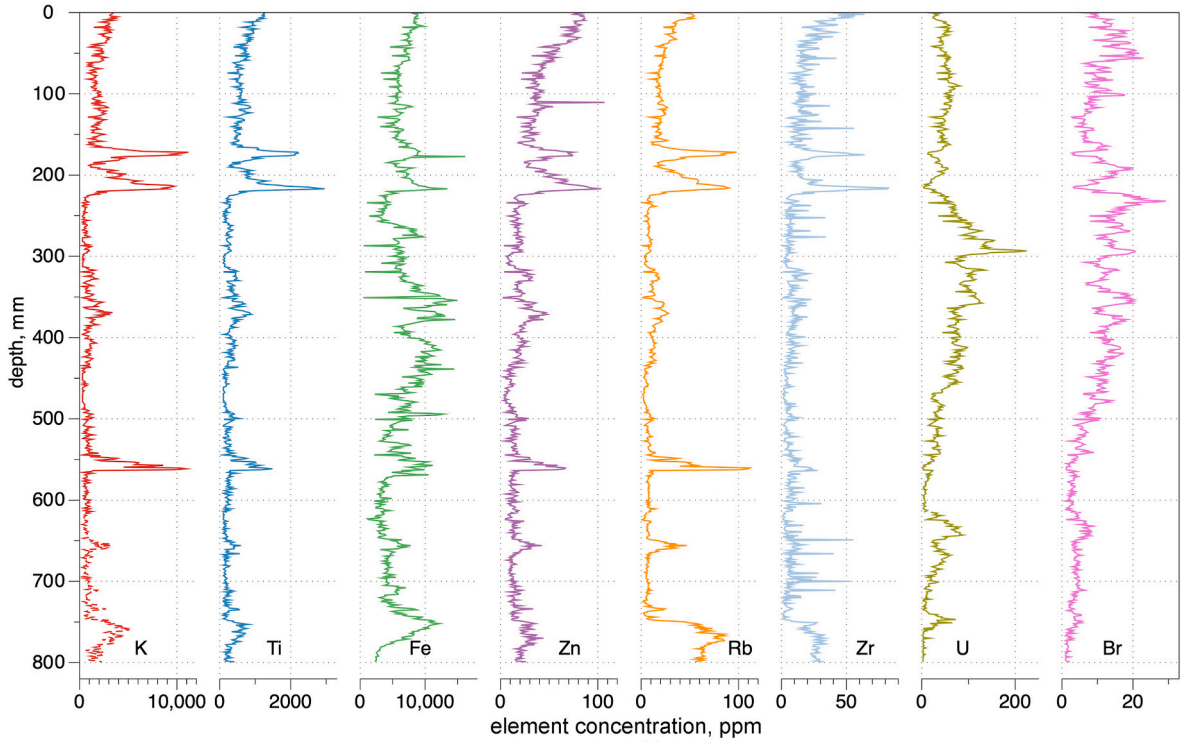


**Fig. 3.** Results of the SR-XRF element analysis. Core Kar-14-1.

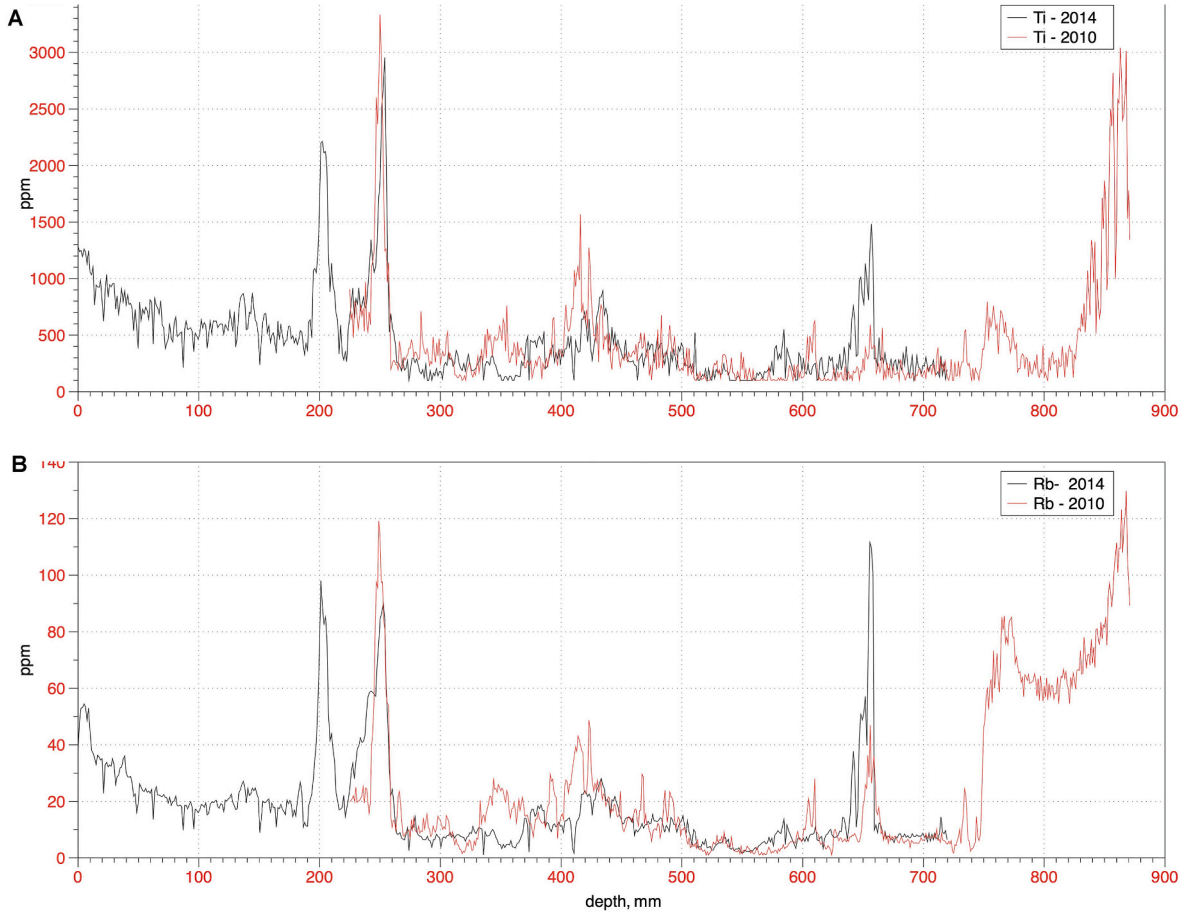


**Fig. 4.** Correlation of cores Kar-10-2 and Kar-14-1 using high resolution titanium (A) and rubidium (B) concentrations from SR-XRF.

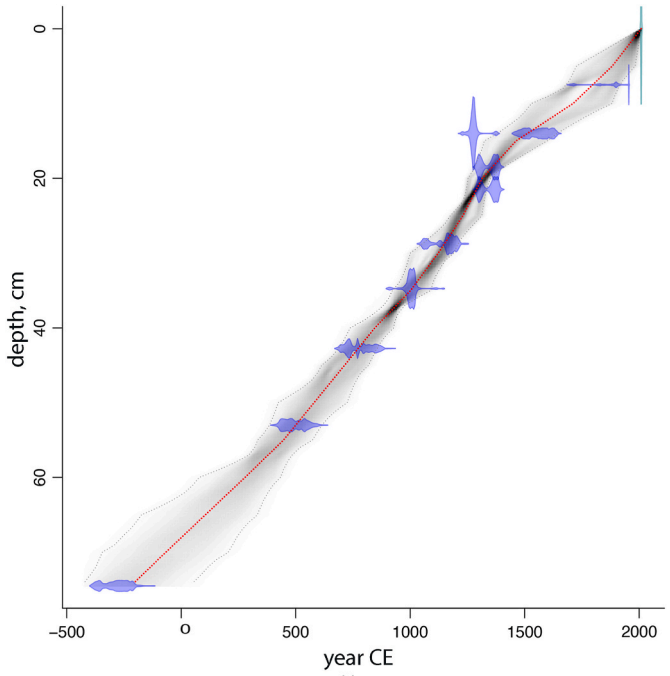


**Fig. 5.** Age-depth model for combined cores Kar-10-2 and Kar-14-1. Created using rBacon routine for R with IntCal20 calibration curve. The shaded region indicates Bayesian age depth uncertainty; the median age distribution is shown with red.

lake. Gilfedder et al. (2011) proposed $Br/C_{org}$ ratio to trace the relative importance of auto-vs. allochthonous input to lakes. Similarly, Guevara et al. (2019) proposed the Br/OM ratio (the ratio of Br to organic matter content evaluated by loss-on-ignition at 550 °C (LOI550)) as a marker of primary autochthonous productivity in a study of a series of deep and shallow lakes. In the case of Lake Karakel, LOI550 yields a relatively constant result around 35–40% with the exception of two dips marking the lowered organic content corresponding to the visible interlayers around the depth 20 and 60 cm. Consequently, the Br/LOI ratio introduced by Guevara et al. (2019) remains relatively constant staying within a 0.2–0.6 range throughout most of the sequence (Fig. 6). We interpret these results as an indicator of the invariable source of organic matter throughout the studied 2000-year period with the exception of the episodes corresponding to increased lithogenic input.

A number of studies have shown correlation between Br concentrations and total organic carbon (TOC) (Guyard et al., 2007; Giralt et al., 2011; Liu et al., 2013; Kalugin et al., 2007). Br was used as an organic tracer in the sedimentary records of lakes of East Siberia (Fedotov et al., 2015; Stepanova et al., 2019). These parameters are known to reflect productivity, what makes Br a temperature-dependent proxy with its concentration in the sediment increasing during warmer periods.

Novel nondestructive sediment core analytical techniques such as μXRF and SR XRF enabled obtaining Br concentration at high resolution. That opened the door to using Br as a proxy for high-resolution paleoclimatic reconstructions. Kalugin et al. (2007) report a correlation between the Br content and annual temperature at the meteorological station of Barnaul during AD 1840–1996 ($r = 0.41$, $p < 0.05$). The authors then used Br content (along with XRD parameter and Sr/Rb ratio) to reconstruct 800-year temperature record in the Altai region.

Our previous study of the upper part of the varved sedimentary sequence of Lake Donguz-Orun (Central Caucasus) showed that Br content in uppermost part of sediment positively correlates with instrumental annual temperature (Br: $r = 0.41$, $p < 0.05$) registered at the proximal weather station (Alexandrin et al., 2018). That witnesses Br being an indicator of both variations in the input of organic matter and/or lake primary productivity.

Our line of evidence of Br content being temperature-sensitive in the case of Lake Karakel sedimentary record is based on the following observation. The initial study of the lake's sediment (Solomina et al., 2014) discovered a correlation between the Br content in the sediment and the content of the broadleaved tree pollen. Broadleaved tree pollen was previously used as an indicator of warm climate in the Caucasus (Serebryanny et al., 1984; Knyazev et al., 1992; Pavlova and Onipchenko, 1992). The composition of broadleaved tree pollen is important, too – the more polydominant the species is, the more it tends to reflect increased heat availability. Decreased heat availability, in turn, can be traced through increased share of conifers due to decreased broadleaf trees. At the same time, a growth in the share of small-leaved tree species in the spectra would rather imply variations in moisture availability. Small-leaved tree species in mountainous environments tend to first colonize the surfaces disturbed by slope processes, and their increased share can, therefore, witness increased slope processes due to higher atmospheric precipitation. The majority of the broadleaved tree pollen in the region is comprised of hornbeam and beech, the species that tend to prefer moist calcareous friable habitats and are generally sensitive to changes in heat availability (Chepurnaya, 2014).

The inferred agreement between the Br curve and the broadleaved tree pollen was preserved when the spore-pollen analysis was performed for the upper part of the core Kar-14-1 (Chepurnaya et al., 2022). Fig. 7A shows the content of the broadleaved tree pollen for the two overlapping cores combined with the Br curve. Noteworthy is the similar long-term variability of the two proxy archives. In order to assess the correlation quantitively we have used a low-pass spline for both datasets: 80-point for Br and 10-point for broadleaved tree pollen. This way the correlation is $r = 0{,}72$; $p < 0.05$ (Fig. 7B).

Given all the aforementioned, we regard the Br curve of the Lake Karakel sediment as an uninterrupted and high-resolution proxy for the variations of heat availability in the Western Caucasus for the past 2000 years. The temporal resolution of our Br curve is around 3 years, remaining relatively constant throughout the whole period. Uncertainties in the uppermost (most recent) part of our Br-derived chronology (see further) do not allow creation of a quantitative temperature reconstruction, yet the time frames of the principal climatic events of that period can be defined precisely.

### 5.2. *Paleoclimatic implications*

In order to confirm the ability of our Br curve to reproduce long-term climatic variability during the last 2000 years we juxtapose it with known temperature reconstructions. Fig. 8 shows the Br curve of Lake Karakel compared with reconstructed mean annual temperature in Europe (multiple proxies; 31-year filtered; PAGES2k Consortium, 2017) and Northern Hemisphere (multiple proxies; annual data; Moberg et al., 2005) and the datasets smoothed with polynomial spline highlighting the long-term temperature variability.

The period of positive temperature anomalies around 1000 CE (marked with yellow shading in the Fig. 8) and the period of negative temperature anomalies around 1600 CE (marked with blue shading in the Fig. 8) are apparent in all the three timeseries. At the same time, certain periods show the discrepancy between our Br curve and temperature reconstructions (marked with red shading in the Fig. 8).

The study of the climate of the Caucasus Mountains has always been interesting in relation to the well-studied Alps. Among other available paleoclimatic tracers there are a number of reconstructions of the glacier variations of the Alps for the Late Holocene. Holzhauser et al. (2005) reconstructed fluctuations of the Great Aletsch, the Gorner and the Lower Grindelwald glaciers in the Swiss Alps during the last 3500 years based on tree-ring width, radiocarbon, archeological and historical data. Variations of the Great Aletsch Glacier with its long length represent a clear smoothed reflection of inter-annual climatic trends (Holzhauser et al., 2005). Here we present the comparison of the Great Aletsch Glacier terminus variations and our Br curve from Lake Karakel (Fig. 9).

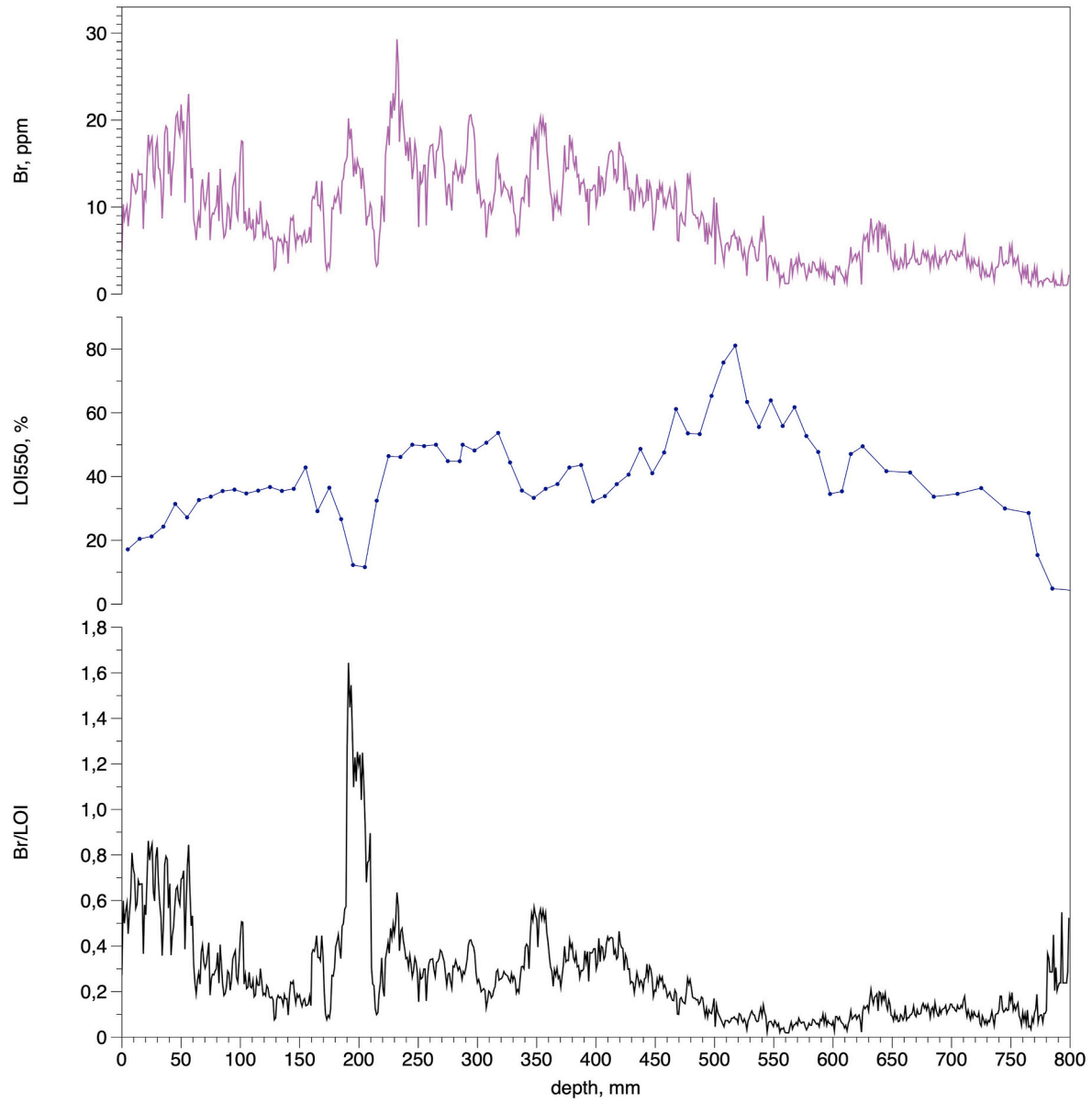


**Fig. 6.** Bromine content in the Lake Karakel sediment, results of the weight loss-on-ignition analysis (LOI550) and the Br/LOI ratio.

The last 1500 years are marked with general accordance of the two timeseries, especially if the time lag of Great Aletsch Glacier in relation to direct climate forcing estimated as few decades (Holzhauser et al., 2005) is taken into account. Cold conditions around 1300-1850 marking the three-phase Little Ice Age in the Great Aletsch chronology generally conform with the lowest values of our Br record during the last 1500 years around 1250–1850 CE. Warm conditions in 750–1200 C E corresponding to the glacier terminus close to the recent (year 2002) position generally conform with the high values of Br in Lake Karakel sediment around 700–1200 C E.

The cooling period from 536 to about 660 CE in the Northern Hemisphere is recognized as the Late Antique Little Ice Age (Büntgen et al., 2016). Advances of alpine glaciers in 5–6 century CE must have been occurring across all the Alps (Holzhauser et al., 2005; Ivy-Ochs et al., 2009; Solomina et al., 2016a) with the biggest equilibrium line altitude depression at least during the first millennium CE (Holzhauser et al., 2005; Le Roy et al., 2015). In the Caucasus no direct evidence of glacier advances of that time is known so far. A series of dated buried soils in the valley of Baksan (Elbus Region) that group around 5–6 century could support glacier advances at the time, but it requires additional study.

The two time series – our Br record and the variations of the Great Aletsch Glacier –show a discrepancy starting from 400 BCE (beginning of the Lake Karakel chronology) till 500 C E (marked with color shading in the Fig. 9). The Lake Karakel proxies for heat availability – both Br and broadleaved tree pollen – indicate cold conditions in the Caucasus during that time. Meanwhile, the period around BCE-CE margin in Europe is widely recognized as the Roman Warm Period (Mann et al., 2009; Moberg et al., 2005; Ljungqvist et al., 2016; etc.). The alpine glaciers at that time had probably reached the position equal to that of the end of the 20-th century (Holzhauser et al., 2005; Joerin et al., 2006).

Interestingly, the notion of possible cold conditions in the Caucasus in the 3–4 century CE is supported by the recent moraine cosmogenic dates of the glacier Irik in the Elbrus Region (Solomina et al., in press): (1570 ± 230 BP, 1630 ± 230 BP, 1680 ± 240 BP) (marked as blue dots with error bars at the Fig. 9). Whether our data in fact indicates cold conditions in the Caucasus prior to 500 C E or the divergence between the records from the Alps and the Caucasus is explained by Lake Karakel's fault signal is a matter of future thorough research that should

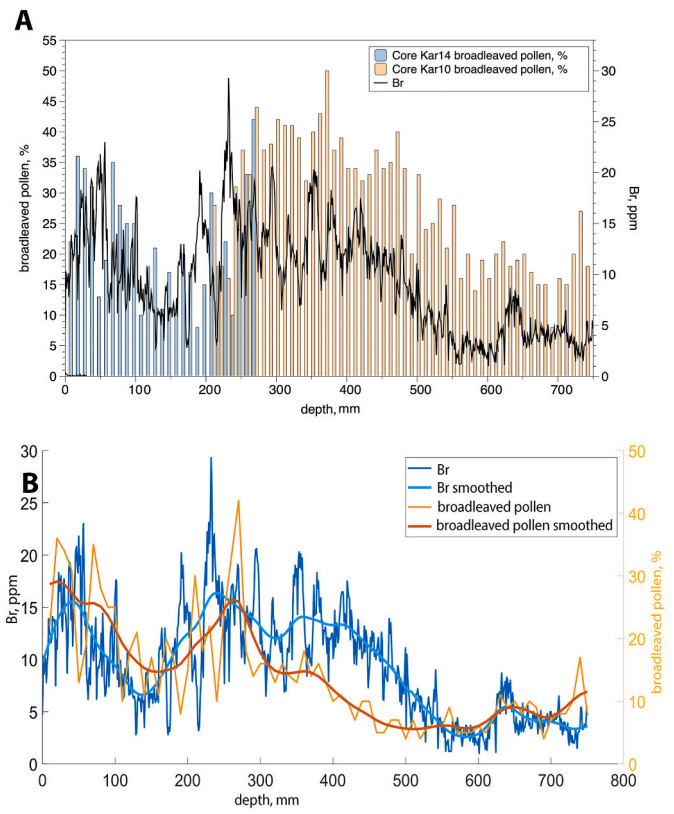


**Fig. 7.** A. Results of the SR-XRF-derived content of bromine in the sediment combined with content of broadleaved tree pollen for the cores Kar-14-1 and Kar-10-2. B. Smoothed values of Br (80-point) and broadleaved tree pollen (10-point).

include other sedimentary archives. For now, we exclude this inapparent period from subsequent paleoclimatic implications of the Lake Karakel Br record.

In order to support the veracity of our 3-year-resolution Br curve for reflecting past temperature variations we compare it with locally available temperature reconstructions. Noteworthy is the comparison with annually-resolved gridded (42.5°N x 42.5°E grid-point) reconstruction of growing season (April–September) temperature for Europe based on tree-rings, historical documentary data, pollen assemblages and ice cores by Guiot et al. (2010) (Fig. 10). A more pronounced agreement with growing season temperature is reasonable since it must be the warm season temperature that is primarily responsible for autochthonous production in Lake Karakel. Both timeseries show the period of positive temperature anomalies in ≈750-1250 C E corresponding to Medieval Climate Anomaly and a tangible cold period in ≈1250-1850 C E corresponding to Little Ice Age.

Duration of Medieval Climate Anomaly in the Caucasus has been a subject for debates since the mid-20-th century. Generally, it falls in the span between 6-th and 12-th centuries CE (Tushinsky, 1964; Turmanina, 1979; Serebryanny et al., 1984). G. Tushinsky (1964) first proposed the so-called "Arkhyz break in glaciation" as a warm period prior to Little Ice Age. Most of the early evidence, though, is based on archeological, historical and palynological data with limited chronological control (Solomina et al., 2016b). The magnitude of warming is also a matter of discussion. Certain sources (e.g., Turmanina, 1979, 1988; Kuznetsov, 1993) propose a warmer-than-present climate in the Caucasus during the mediaeval. Our continuous curve could have shed light on the question of magnitude of Medieval Climate Anomaly (MCA) warming, but the disturbed climate signal in the 20-th century portion (see further) restricts such estimates, since we are unable to calibrate our data against the meteorological observations. Medieval Climate Anomaly in our data is distinguished not only with the magnitude but also with the abruptness of change to warmer conditions in the mid-10th century and to colder conditions in the mid-13th.

The period from the mid-13th till the mid-19th centuries CE marked with negative temperature anomalies according to our Br curve (Fig. 10)

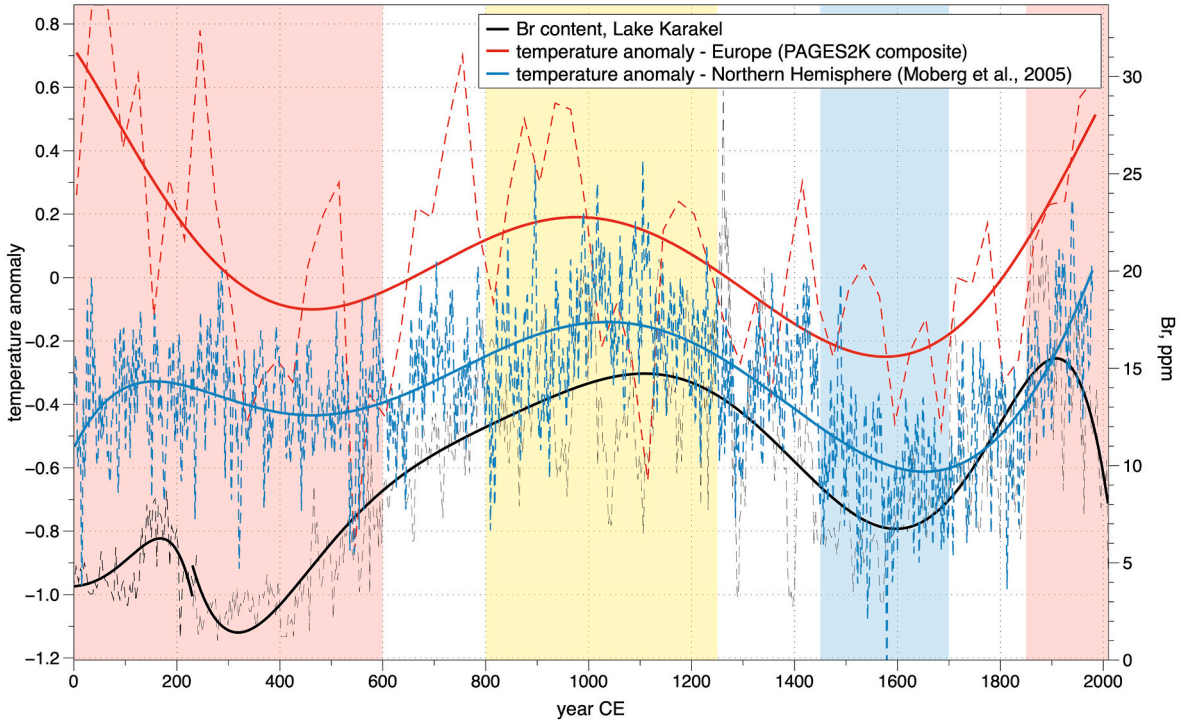


**Fig. 8.** Comparison of bromine content in the Lake Karakel sediment (this study) with reconstructed annual temperature for Europe (PAGES2k Consortium, 2017) and Northern Hemisphere (Moberg et al., 2005); solid lines represent the values smoothed with polynomial spline. For details of color shading see text.

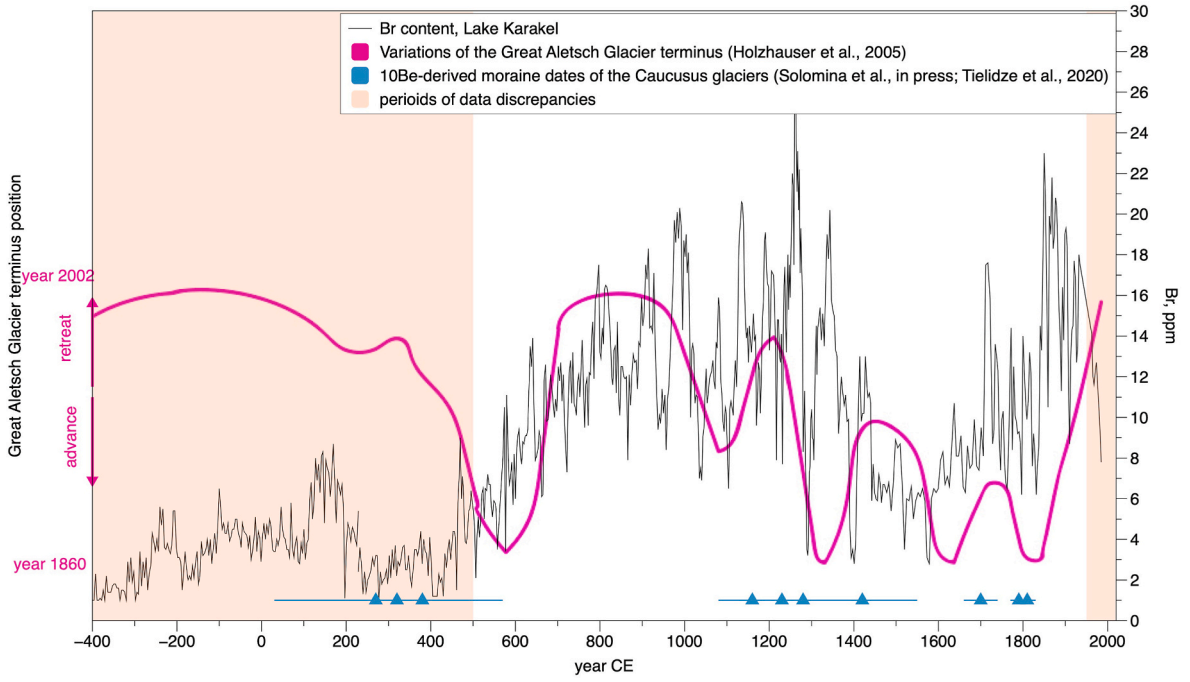


**Fig. 9.** Comparison of bromine content in Lake Karakel sediment (this study) with the curve of the variations of the Great Aletsch Glacier terminus (Holzhauser et al., 2005) and cosmogenic moraine dates of the glaciers Irik, Kashkatash (Elbrus Region, Caucasus) (Solomina et al., in press) and Chalaati (Georgian Caucasus) (Tielidze et al., 2020).

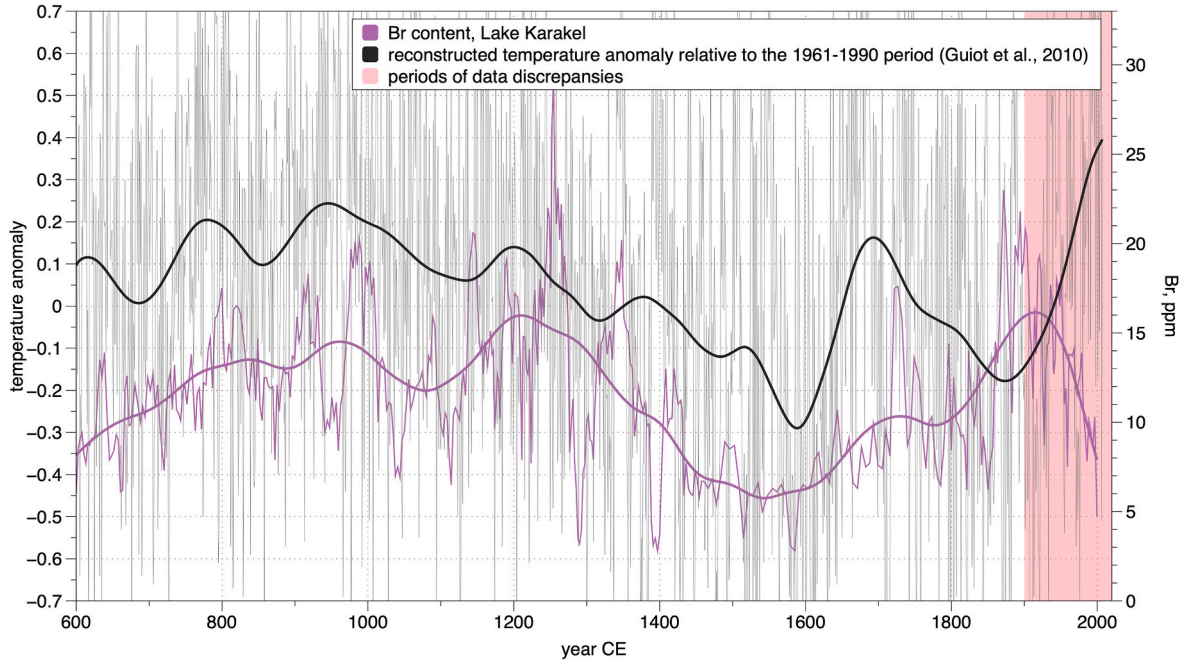


**Fig. 10.** Comparison of bromine content in Lake Karakel sediment (this study) with reconstructed temperature of the growing season (April–September) in Europe for the past 1400 years – grid-point 42.5°N x 42.5° E (Guiot et al., 2010); solid lines: smoothing with local regression.

generally corresponds with a contemporary conception of the time frames of the Little Ice Age in Europe (IPCC AR5, 2013). The amount of the LIA evidence in the Caucasus is more abundant as compared to such for the MCA, but decreases back in time. A glacial advance centered around 13th century regarded as the LIA 1st stage was reported by Serebryanny et al. (1984) and Zolotarev and Seinova (1988) with the use of lichenometry and buried $^{14}C$ buried soil dating. Glacial advance of 15–16th centuries (LIA 2nd stage) could have had a smaller magnitude compared to such 13th and 19th centuries and are thus poorly constrained. Still, certain evidence exists, like the oldest tree dating to 1598 C E on the moraine of the Bol'shoy Azau Glacier (Solomina et al., 2016b). The question as to the advance of 13th century has been larger than the advance of the last stage of LIA was raised by Serebryanny et al. (1984) and Zolotarev and Seinova (1988). Recent findings based on cosmogenic ($^{10}Be$) dating of glacier moraines in Western and Central Caucasus (Solomina et al., in press) provide evidence that the glacier

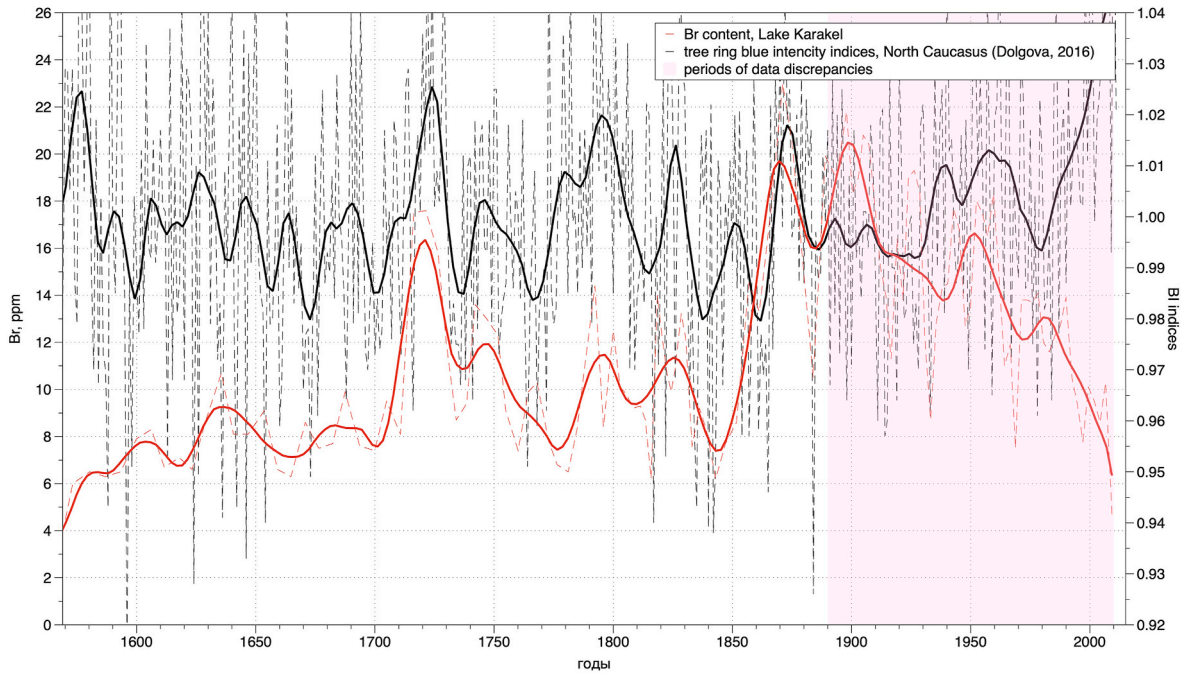


**Fig. 11.** Comparison of bromine content in Lake Karakel sediment (this study) with June–September temperature reconstruction in the Northern Caucasus based on blue intensity data (Dolgova, 2016); solid lines: smoothing with local regression.

advance of the LIA 1st stage could have exceeded the advance of the LIA 3$^{d}$ stage, but only by a small fraction.

Comparison between the cold episodes indicated by the Br curve and the known LIA advances of the glaciers in the Caucasus provides additional confirmation. For the Kashkatash Glacier in the Elbrus Region eight $^{10}$Be moraine dates are known. Four of them cluster around the age 700–820 BP (1130–1250 CE) with 100–170-year errors with an additional date of 530 ± 130 BP (1420 ± 130 CE) (Solomina et al., in press). In the Georgian Caucasus Chalaati Glacier moraines are dated to 790 ± 80 and 670 ± 100 BP (1160 ± 80 and 1280 ± 100 CE) (Tielidze et al., 2020). These advances most likely represent the first stage of the LIA and are in general agreement with the two-fold LIA 1st stage marked by our Br curve. Recent advances of the Kashkatash Glacier are dated to 1700–1810 C E. Advances of the Caucasus glaciers are shown with blue dots with error bars at the Fig. 9.

Other important evidence comes from the recent studies of the buried soils in the vicinity of the Bolshoy Azau Glacier of Mt Elbrus (Solomina et al., 2022). According to this research, the glacier reached its maximum thickness during two advances in 19th and 17th centuries interrupted by a short warming in the Little Ice Age, as well as in the 7th century CE, in the Late Antique Little Ice Age, and shortly before 2800–2900 BP. Glacier retreat during the two long intervals allowed the development of 15–20 cm thick soil profiles during the Medieval Climatic Anomaly.

For the Northern Caucasus, the only continuous high-resolution temperature reconstruction that was available so far is the June–September temperature reconstruction based on blue intensity tree-ring data by E. Dolgova (2016) covering the period 1569–2011 C E. The blue intensity chronology strongly correlates with the mean June–September temperature ($R = 0.74$; $p < 0.05$) from the weather station "Kluhorskij Pereval".

Despite our Br chronology is being based on radiocarbon age-depth model and therefore climatic events may shift along the time axis within dates' confidence limits, the main trends of decadal temperature variability are replicated by both timeseries (Fig. 11). Noteworthy is the convergence of warm periods in the 1730s, 1790s, 1830s and 1870-s. Minimums in the two timeseries coincide with the dated glacier advances in the Caucasus in the 18th and 19th centuries (Bushueva, 2013; Solomina et al., 2016b).

Comparison of our Br curve with dendrochronological reconstruction of the warm season temperature provides the evidence that bromine content in the sediment is capable of tracing not only the long-term, but also short-term climatic variability, what is especially valuable while creating high-resolution reconstructions.

20th century is marked by discrepancy between our Br curve and all the reconstructions – both global and regional (marked with color shading at (Figs. 8–11)). Warming in the 20th century is finely reproduced by tree rings and other proxies, but not by the bromine content of the Lake Karakel sediment. The nature of such divergence might be found in anthropogenic disturbance of the lake and lake's catchment area at the time. Development of the Teberda region started in the end of 19th century (1868 – the settlement founded, 1894–1903 – Sukhum military road constructed, 1925 – first health resort opened). With the lake situated practically in the middle of the settlement, the fault in the Br signal in the uppermost part of the sediment is most likely connected with construction-related pollution of the 20th century. Gilfedder et al. (2011) showed such a dilution effect where autochthonous (organic) material with high bromine concentrations is diluted by mineral sediments from the catchment. Unfortunately, this discrepancy means that: (1) we are unable to assess the magnitude of the MCA warming in the Caucasus as compared to the current warming – a question that has been long debated; (2) we are unable to calibrate the Br content of the Lake Karakel sediment against the instrumental records and thus create a continuous qualitative temperature reconstruction. These are the issues that have to be addressed in the future with the use of other sedimentary archives of the Caucasus region.

Comparison of the Br curve with potential forcing factors – volcanic activity (Toohey and Sigl, 2017) and total solar irradiance (Wu et al., 2018) reveal no direct connection with these parameters. For the volcanic activity it is reasonable – despite the fact that the resolution of our chronology is high, it is still insufficient to trace high-frequency signals lasting several years. Smoothed curve of decadal values of total solar irradiance reveals certain resemblance with the smoothed curve of bromine in the Lake Karakel sediment throughout the last millennium with a pronounced minimum in the mid-LIA. The possible relation between the sedimentary bromine and solar forcing is a matter of future

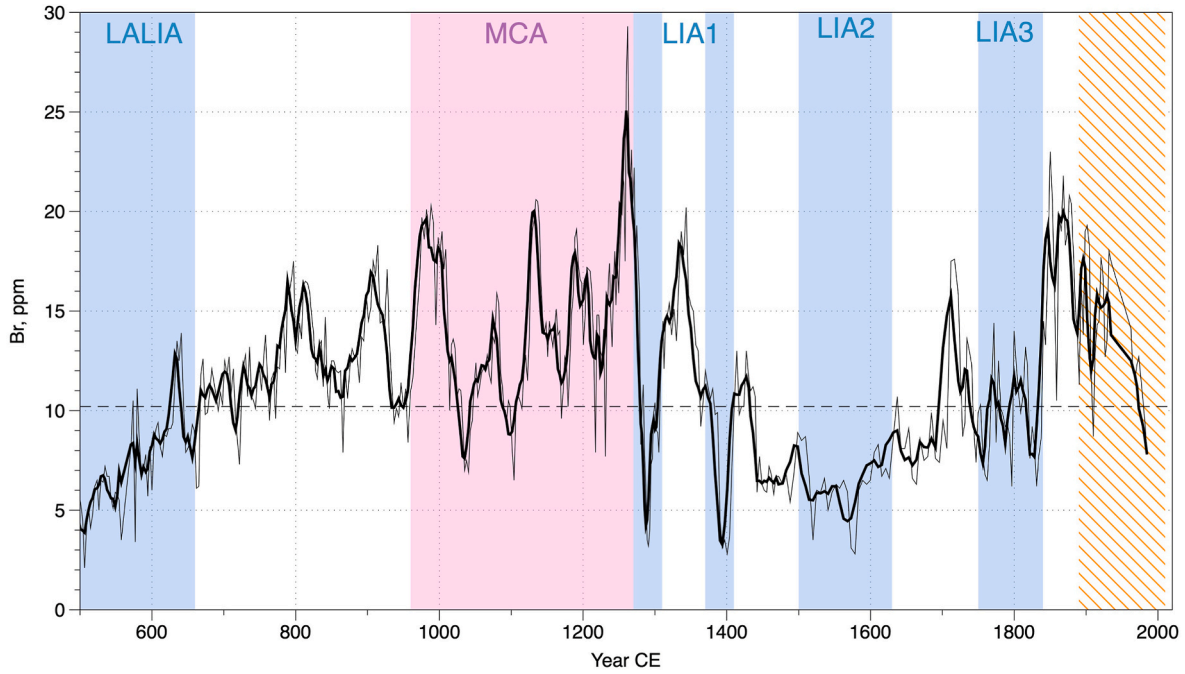


**Fig. 12.** The curve of bromine content in the sediment of Lake Karakel as a proxy for variations of heat availability in the Western Caucasus. Solid line: 4-point moving average, dashed line: mean value of Br in the last 1500 years. Dashed line: average value of Br within a 1500-year period. Blue shading: cold periods, red shading: warm period, color hatching: period of data discrepancies (see text).

research.

Given all the above-mentioned, we interpret our Br curve as representing a continuous high-resolution indicator for variations of heat availability in the Western Caucasus for the past 1500 years (excluding the 20th century). Fig. 12 shows the Br curve and its 4-point (12-year) moving average that we used to determine the time frames of the main climatic events. According to our data, Late Antique Little Ice Age lasted until ca. 660 C E. Medieval Climate Anomaly (also called Arkhyz break in glaciation in the Caucasus) lasted from the mid-9th century (ca. 960 CE) till the mid-13th century (ca. 1270 CE). At this time the temperature could have risen close to the present-day level. The period from the mid-13th till the mid-19th centuries is generally marked with negative Br anomalies. Within it we distinguish three stages of Little Ice Age in the Western Caucasus: a two-fold LIA 1st stage (ca. 1270–1310 and 1370–1410), at this time glacier advance in the region could have reached its maximum in the past 1500 years; LIA 2nd stage (ca. 1500–1630) – and a well-documented LIA 3d stage (ca. 1750–1840).

## 6. Conclusions

- Combination of SR-XRF analysis, radiocarbon dating and lithostratigraphic analysis allowed for creating a complete high-resolution sedimentary record covering the past two millennia.
- Concentration of bromine in the bottom sediment can be used as a proxy for past temperature changes since Br is connected to lake's productivity. This notion is supported by coherent behavior of our Br curve and concentration of broadleaved tree pollen, a parameter also known to be temperature-dependent. We thus interpret our Br curve as a marker for the variations of heat availability in the Western Caucasus.
- Our Br curve shows consistent agreement with hemispheric, regional and local temperature reconstructions for the last 1500 years (excluding 20th-21st centuries).
- Basing on our Br curve we distinguish the time frames of the following climatic events in the region: MCA (ca. 960–1270 CE); LIA 1st stage (ca. 1270–1310 and 1370–1410); LIA 2nd stage (ca. 1500–1630); LIA 3d stage (ca. 1750–1840).
- The magnitude of the MCA warming cannot be quantitatively assessed basing on our record, LIA 1 could have been the coldest time during the past 1500 years (supported by moraine dating), though the magnitude of cooling is comparable to the other stages of LIA.

## Author contributions

MA is responsible for paleoclimatic research based on high-resolution sedimentary studies in the IG RAS, Moscow; he took part in sediment coring of Lake Karakel, preparation for sedimentary analyses, data analysis and writing. OS is a leader of the paleoclimatic research group in the IG RAS who provided paleoclimatic implications and consulting. AD performed the SR XRF analysis in the IGM SB RAS, Novosibirsk.

## Data availability

The results of the SR XRF analysis are presented in the Supplementary material. All the other data are available upon request from the corresponding author M.Y. Alexandrin.

## Declaration of competing interest

The authors declare that they have no known competing financial interests or personal relationships that could have appeared to influence the work reported in this paper.

## Acknowledgments

This work was supported by the State Target Project of the Institute of Geography RAS No. 0127-2019-0008 (field works), Megagrant project (agreement № 075-15-2021-599, 8.06.2021) (data analysis and writing) and the Kazan Federal University Strategic Academic Leadership Program (PRIORITY-2030) (analytical works, dating). The authors thank Vladimir Matskovsky, Vasily Shishkov, and Vladimir Mikhalenko for the assistance in the coring process, Ivan Kalugin for assistance with SR XRF analysis, Anna Chepurnaya ana Elena Novenko for results of the

spore-pollen analysis.

## Appendix A. Supplementary data

Supplementary data to this article can be found online at https://doi.org/10.1016/j.quaint.2023.05.020.

## References


Addison, J.A., Finney, B.P., Jaeger, J.M., Stoner, J.S., Norris, R.D., Hangsterfer, A., 2013. Integrating satellite observations and modern climate measurements with the recent sedimentary record: an example from Southeast Alaska. J. Geophys. Res.: Oceans 118 (7), 3444–3461.

Alexandrin, M.Y., Darin, A.V., Kalugin, I.A., Dolgova, E.A., Grachev, A.M., Solomina, O. N., 2018. Annual sedimentary record from Lake Donguz-Orun (Central Caucasus) constrained by high resolution SR-XRF analysis and its potential for climate reconstructions. Front. Earth Sci. 6, 158.

Bahr, A., Jiménez-Espejo, F.J., Kolasinac, N., Grunert, P., Hernández-Molina, F.J., Röhl, U., et al., 2014. Deciphering bottom current velocity and paleoclimate signals from contourite deposits in the G ulf of C ádiz during the last 140 kyr: an inorganic geochemical approach. G-cubed 15 (8), 3145–3160.

Blaauw, M., Christen, J.A., 2011. Flexible paleoclimate age-depth models using an autoregressive gamma process. Bayesian Anal. 6 (3), 457–474.

Büntgen, U., Myglan, V.S., Ljungqvist, F.C., McCormick, M., Di Cosmo, N., Sigl, M., et al., 2016. Cooling and societal change during the late Antique Little ice age from 536 to around 660 AD. Nat. Geosci. 9 (3), 231–236.

Bushueva, I.S., 2013. Kolebaniya Lednikov Na Tsentralnom I Zapadnom Kavkaze Po Kartograficheskim, Istoricheskim I Bioindikacionnim Dannim Za Poslednie 200 Let (Fluctuations of Glaciers on the Central and Western Caucasus Using Cartographical, Historical and Proxy Data over the Last 200 Years). (Ph.D. thesis) Institute of Geography Russian Academy of Sciences, Russia (In Russian).

Chepurnaya, A.A., 2014. Dynamics of vegetation cover in the late Holocene in Lake Karakel – Teberda Valley area (according to palynological data). Bull. Russ. Acad. Sci. No 2, 84–95 (In Russian).

Chepurnaya, A.A., Novenko, E.Y., Aleksandrin, M.Y., 2022. Late Holocene vegetation history of the Western Caucasus inferred from high-resolution pollen record from Lake Karakel. Limnology and Freshwater Biology 1408–1411.

Croudace, I.W., Rothwell, R.G. (Eds.), 2015. Micro-XRF Studies of Sediment Cores: Applications of a Non-destructive Tool for the Environmental Sciences, vol. 17. Springer.

Darin, A.V., Kalugin, I.A., Rakshun, Y.V., 2013. Scanning X-ray microanalysis of bottom sediments using synchrotron radiation from the BINP VEPP-3 storage ring. Bull. Russ. Acad. Sci. 77, 182–184.

Darin, A.V., Rakshun YaV, R., 2013. Determination procedure of the elemental composition of rock samples by x-ray fluorescence using synchrotron radiation from the VEPP-3 storage device. Nauchn. Vestn. Novosib. Gos. Tekhn. Univ 2 (51), 112–118.

Dean, W.E., 1974. Determination of carbonate and organic matter in calcareous sediments and sedimentary rocks by loss on ignition: comparison with other methods. J. Sediment. Res. 44, 242e248.

Dolgova, E., 2016. June–September temperature reconstruction in the Northern Caucasus based on blue intensity data. Dendrochronologia 39, 17–23.

Fedotov, A.P., Trunova, V.A., Enushchenko, I.V., Vorobyeva, S.S., Stepanova, O.G., Petrovskii, S.K., et al., 2015. A 850-year record climate and vegetation changes in East Siberia (Russia), inferred from geochemical and biological proxies of lake sediments. Environ. Earth Sci. 73 (11), 7297–7314.

Gilfedder, B.S., Petri, M., Wessels, M., Biester, H., 2011. Bromine species fluxes from Lake Constance's catchment, and a preliminary lake mass balance. Geochem. Cosmochim. Acta 75 (12), 3385–3401.

Giralt, S., Rico-Herrero, M.T., Vega, J.C., Valero-Garcés, B.L., 2011. Quantitative climate reconstruction linking meteorological, limnological and XRF core scanner datasets: the Lake Sanabria case study, NW Spain. J. Paleolimnol. 46 (3), 487–502.

Grachev, A.M., Novenko, E.Y., Grabenko, E.A., Alexandrin, M.Y., Zazovskaya, E.P., Konstantinov, E.A., et al., 2020. The Holocene paleoenvironmental history of western caucasus (Russia) reconstructed by multi-proxy analysis of the continuous sediment sequence from Lake Khuko. Holocene, 0959683620972782.

Guevara, S.R., Rizzo, A., Daga, R., Williams, N., Villa, S., 2019. Bromine as indicator of source of lacustrine sedimentary organic matter in paleolimnological studies. Quat. Res. 92 (1), 257–271.

Guiot, J., Corona, C., ESCARSEL members, 2010. Growing season temperatures in Europe and climate forcings over the past 1400 years. PloS one 5 (4), e9972.

Guyard, H., Chapron, E., St-Onge, G., Anselmetti, F.S., Arnaud, F., Magand, O., et al., 2007. High-altitude varve records of abrupt environmental changes and mining activity over the last 4000 years in the Western French Alps (Lake Bramant, Grandes Rousses Massif). Quat. Sci. Rev. 26 (19–21), 2644–2660.

Heiri, O., Lotter, A.F., Lemcke, G., 2001. Loss on ignition as a method for estimating organic and carbonate content in sediments: reproducibility and comparability of results. J. Paleolimnol. 25, 101e110.

Holzhauser, H., Magny, M., Zumbuühl, H.J., 2005. Glacier and lake-level variations in west-central Europe over the last 3500 years. Holocene 15 (6), 789–801.

Ivy-Ochs, S., Kerschner, H., Maisch, M., Christl, M., Kubik, P.W., Schlüchter, C., 2009. Latest pleistocene and Holocene glacier variations in the European Alps. Quat. Sci. Rev. 28 (21–22), 2137–2149.

Joerin, U.E., Stocker, T.F., Schlüchter, C., 2006. Multicentury glacier fluctuations in the Swiss Alps during the Holocene. Holocene 16 (5), 697–704.

Kandasamy, S., Lin, B., Lou, J.Y., Kao, S.J., Chen, C.T.A., Mayer, L.M., 2018. Estimation of marine versus terrigenous organic carbon in sediments off southwestern Taiwan using the bromine to total organic carbon ratio as a proxy. J. Geophys. Res.: Biogeosciences 123 (10), 3387–3402.

Kalugin, I., Astakhov, A., Darin, A., Aksentov, K., 2015. Anomalies of bromine in the estuarine sediments as a signal of floods associated with typhoons. Chin. J. Oceanol. Limnol. 33 (6), 1489–1495.

Kalugin, I., Daryin, A., Smolyaninova, L., Andreev, A., Diekmann, B., Khlystov, O., 2007. 800-yr-long records of annual air temperature and precipitation over southern Siberia inferred from Teletskoye Lake sediments. Quat. Res. 67 (3), 400–410.

Knyazev, A.V., Savinetsky, A.B., Gei, N.A., 1992. History of north Osetia vegetation during the Holocene. In: Dinesman, L.G. (Ed.), Historical Ecology of Wild and Domestic Ungulates. Nauka Press, Moscow, pp. 84–108 (In Russian).

Kutuzov, S., Legrand, M., Preunkert, S., Ginot, P., Mikhalenko, V., Shukurov, K., et al., 2019. The Elbrus (Caucasus, Russia) ice core record–Part 2: history of desert dust deposition. Atmos. Chem. Phys. 19 (22), 14133–14148.

Kuznetsov, V.A., 1993. Alano-osetinskie Etyudy (Alan-Osetian Studies). Izdatelstvo Severo-Osetinskogo instituta gumanitarnyh issledovaniy, Vladikavkaz (In Russian).

Kvavadze, E.V., Efremov, Y.V., 1996. Palynological studies of lake and lake-swamp sediments of the Holocene in the high mountains of Arkhyz (Western Caucasus). Acta Palaeobot. 36, 107–120.

Le Roy, M., Nicolussi, K., Deline, P., Astrade, L., Edouard, J.L., Miramont, C., Arnaud, F., 2015. Calendar-dated glacier variations in the western European Alps during the neoglacial: the mer de Glace record, Mont Blanc massif. Quat. Sci. Rev. 108, 1–22.

Leri, A.C., Hakala, J.A., Marcus, M.A., Lanzirotti, A., Reddy, C.M., Myneni, S.C.B., 2010. Natural organobromine in marine sediments: new evidence of biogeochemical Br cycling. Global Biogeochem. Cycles 24.

Leri, A.C., Myneni, S.C.B., 2012. Natural organobromine in terrestrial ecosystems. Geochem. Cosmochim. Acta 77, 1–10.

Liu, X., Colman, S.M., Brown, E.T., Minor, E.C., Li, H., 2013. Estimation of carbonate, total organic carbon, and biogenic silica content by FTIR and XRF techniques in lacustrine sediments. J. Paleolimnol. 50 (3), 387–398.

Ljungqvist, F.C., Krusic, P.J., Sundqvist, H.S., Zorita, E., Brattström, G., Frank, D., 2016. Northern Hemisphere hydroclimate variability over the past twelve centuries. Nature 532 (7597), 94–98.

Mann, M.E., Zhang, Z., Rutherford, S., Bradley, R.S., Hughes, M.K., Shindell, D., et al., 2009. Global signatures and dynamical origins of the Little ice age and Medieval climate anomaly. Science 326 (5957), 1256–1260.

Mayer, L.M., Schick, L.L., Allison, M.A., Ruttenberg, K.C., Bentley, S.J., 2007. Marine vs. terrigenous matter in Louisiana coastal sediments: the uses of bromine:organic carbon ratios. Mar. Chem. 107, 244–254.

Mayer, L.M., Macko, S.A., Mook, W.H., Murray, S., 1981. The distribution of bromine in coastal sediments and its use as a source indicator for organic matter. Org. Geochem. 3 (1–2), 37–42.

Moberg, A., Sonechkin, D.M., Holmgren, K., Datsenko, N.M., Karlén, W., 2005. Highly variable Northern Hemisphere temperatures reconstructed from low-and high-resolution proxy data. Nature 433 (7026), 613–617.

Nesje, A., 1992. A piston corer for lacustrine and marine sediments. Arct. Alp. Res. 24 (3), 257–259.

PAGES2k Consortium, 2017. A global multiproxy database for temperature reconstructions of the Common Era. Sci. Data 4.

Pavlova, I.V., Onipchenko, V.G., 1992. Dynamics of alpine vegetation of the North-western Caucasus during the Holocene. In: Historical Ecology of Wild and Domestic Ungulates. History of the Pasture Systems. Nauka Press, Moscow, pp. 109–129 (In Russian).

Phedorin, M.A., Goldberg, E.L., Grachev, M.A., Levina, O.L., Khlystov, O.M., Dolbnya, I. P., 2000. The comparison of biogenic silica, Br and Nd distributions in the sediments of Lake Baikal as proxies of changing paleoclimates of the last 480 kyr. Nucl. Instrum. Methods Phys. Res. Sect. A Accel. Spectrom. Detect. Assoc. Equip. 448 (1–2), 400–406.

Ramsey, C.B., 2009. Bayesian analysis of radiocarbon dates. Radiocarbon 51 (1), 337–360.

Reimer, P.J., Austin, W.E., Bard, E., Bayliss, A., Blackwell, P.G., Ramsey, C.B., et al., 2020. The IntCal20 Northern Hemisphere radiocarbon age calibration curve (0–55 cal kBP). Radiocarbon 62 (4), 725–757.

State Geological Map of the Russian Federation, scale of 1:100,000 (third edition). Scythian Series. Sheet K-37 (Sochi), K-38 (Mahachkala), k-39, 2011. Izd-vo kartfabriki VSEGEI, St. Petersburg.

Solomina, O.N., Jomelli, V., Bushueva, I.S. European Glacial Landscapes III: the Holocene. The Impact of Climate Change on Glaciers and the Glacial Landscape of Europe during the Last 11,700 Years: a Preliminary Geochronology. Chapter 19. Holocene glacier variations in the Northern Caucasus, Russia, in press.

Solomina, O.N., Bradley, R.S., Hodgson, D.A., Ivy-Ochs, S., Jomelli, V., Mackintosh, A.N., et al., 2015. Holocene glacier fluctuations. Quat. Sci. Rev. 111, 9–34.

Solomina, O.N., Bradley, R.S., Jomelli, V., Geirsdottir, A., Kaufman, D.S., Koch, J., et al., 2016a. Glacier fluctuations during the past 2000 years. Quat. Sci. Rev. 149, 61–90.

Solomina, O.N., Kalugin, I.A., Darin, A.V., Chepurnaya, A.A., Alexandrin, M.Y., Kuderina, T.M., 2014. Ispol'zovaniye geokhimicheskogo i pyl'tsevogo analizov otlozheniy oz. Karakel'dlya rekonstruktsii klimaticheskikh izmeneniy v doline r. Teberda (Severnyy Kavkaz) v pozdnem golotsene: vozmozhnosti i ogranicheniya the implementation of geochemical and palynological analyses of the sediment core of Lake Karakyol for reconstructions of climatic changes in the valley of Teberda River (Northern Caucasus) during the Late Holocene: possibilities and restrictions. Vopr. Geogr. 137, 234–266.

Solomina, O., Bushueva, I., Dolgova, E., Jomelli, V., Alexandrin, M., Mikhalenko, V., et al., 2016b. Glacier variations in the Northern Caucasus compared to climatic reconstructions over the past millennium. Global Planet. Change 140, 28–58.

Stepanova, O.G., Trunova, V.A., Osipov, E.Y., Kononov, E.E., Vorobyeva, S.S., Parkhomchuk, E.V., et al., 2019. Glacier dynamics in the southern part of East Siberia (Russia) from the final part of the LGM to the present based on from biogeochemical proxies from bottom sediments of proglacial lakes. Quat. Int. 524, 4–12.

Serebryanny, L.R., Golodkovskaya, N.A., Orlov, A.V., Malyasova, E.S., Il'ves, E.O., 1984. Kolebaniya Lednikov I Protsessy Morenonakopleniya Na Tsentral'nom Kavkaze (Glacier variations and moraine accumulation: processes in Central Caucasus).

Solomina, O.N., Alexandrovskiy, A.L., Zazovskaya, E.P., Konstantinov, E.A., Shishkov, V. A., Kuderina, T.M., Bushueva, I.S., 2022. Late-holocene advances of the Greater Azau Glacier (Elbrus area, Northern Caucasus) revealed by 14C dating of paleosols. Holocene 32 (5), 468–481.

Tielidze, L.G., Solomina, O.N., Jomelli, V., Dolgova, E.A., Bushueva, I.S., Mikhalenko, V. N., et al., 2020. Change of Chalaati Glacier (Georgian Caucasus) since the little ice age based on dendrochronological and Beryllium-10 data. Ice Snow (3), 453–470.

Toohey, M., Sigl, M., 2017. Volcanic stratospheric sulfur injections and aerosol optical depth from 500 BCE to 1900 CE. Earth Syst. Sci. Data 9 (2), 809–831.

Turmanina, V.I., 1979. Dendrohronologiya lavin v verhov'yah Baksanskoy dolini (Dendro- chronology of avalanches in the upstream of Baksan valley). In: Tushinskiy, G.K. (Ed.), Ritmi Glyatsiologicheskih Protsessov. (Rhythms of Glaciological Processes). MGU Press, Moscow, pp. 128–134 (In Russian).

Turmanina, V.I., 1988. Otsenka klimaticheskikh izmeneniy fitoindikatsionnimi metodami [Climate change estimation using phytoindication]. In: Kolebaniya Klimata Za Poslednee Tysyacheletie [Climate Fluctuations in the Past Millennium. Gidrometeoizdat, Leningrad, pp. 144–145 (in Russian).

Tushinsky, G.K., 1964. Arhyzskij pereryv v oledenenii i lavinnoj dejatel'nosti na Kavkaze v pervom tysjacheletii (Arkhyz break in glaciation and avalanche activity in the Cauca- sus in the first millenim CE). In: Informatsionniy Sbornik O Rabotah Po Mejdunarodnomu Geofizicheskomu Godu (Informational Collection on the Studies of the International Geophysical Year). Publisher, Moscow, pp. 96–101 (In Russian), 10.

Wishkerman, A., Gebhardt, S., McRoberts, C.W., Hamilton, J.T., Williams, J., Keppler, F., 2008. Abiotic methyl bromide formation from vegetation, and its strong dependence on temperature. Environ. Sci. Technol. 42 (18), 6837–6842.

Wu, C.J., Usoskin, I.G., Krivova, N., Kovaltsov, G.A., Baroni, M., Bard, E., Solanki, S.K., 2018. Solar activity over nine millennia: a consistent multi-proxy reconstruction. Astron. Astrophys. 615, A93.

Ziegler, M., Jilbert, T., de Lange, G.J., Lourens, L.J., Reichart, G.J., 2008. Bromine counts from XRF scanning as an estimate of the marine organic carbon content of sediment cores. G-cubed 9 (5).

Zolotarev, E.A., Seinova, I.B., 1988. Oledenenie Elbrusa i ego izverzhenie v golotsene (Gla-ciation of the Elbrus and its eruption in the Holocene). Materialy Glyatsiologicheskikh Issledovaniy 64, 95–101 (in Russian).